SPACE SCIENCE SERIES

10 February 1997

INVOICE

To: Dr. D. Crisp
JPL, MS 241-105
4800 Oak Grove Drive
Pasadena, CA 91109

For final page charges for the *Taylor et al.* chapter in *Venus II*

26 pages at $41.25 per page/3 **$357.50**

Now due: $357.50

You have been charged the surcharge rate for submitting your materials without **Series** template.

Make check payable to: **Venus II**

Mail check to: **Venus II**
P.O. Box 44221
Tucson, AZ 85733

Near-Infrared Sounding of the Lower Atmosphere of Venus

F.W. Taylor[1], D. Crisp[2], and B. Bézard[3].

[1] University Of Oxford, Department Of Physics
Atmospheric, Oceanic & Planetary Physics,
Clarendon Laboratory, Parks Road, Oxford OX1 3PU, England.

[2] Earth and Space Science Division,
Jet Propulsion Laboratory,
4800 Oak Grove Drive,
Pasadena,
California 91109.

[3] DESPA,
Observatoire de Paris,
92195 Meudon,
France.

A book chapter submitted to *Venus 2*

(University of Arizona Press, Tucson, AZ)

January 1996

Address all correspondence to Professor F.W. Taylor at:
Atmospheric, Oceanic & Planetary Physics,
Clarendon Laboratory, Parks Road, Oxford OX1 3PU, England.

Tel: +44 1865 272903

Fax: +44 1865 272924

email f.taylor1@physics.oxford.ac.uk

Abstract

The recent discovery of near-infrared (near-IR) emission from the nightside of Venus provides a powerful new technique for studying its lower atmosphere and surface. This emission is most intense within spectral 'windows' between strong molecular absorption bands in the 0.9 to 2.5 μm wavelength region. The resulting emission from the planet is most easily detected on the nightside, where it is not overwhelmed by the more intense solar flux reflected from the clouds. Near-IR imaging and spectroscopic observations of this emission by ground-based and spacecraft instruments have been used to investigate cloud particle sizes and optical thickness, the winds within the middle and lower cloud decks, and the abundances of several important trace gases, including water vapor, halides, carbon monoxide, sulfur dioxide, and carbonyl sulfide. They have provided new information about the near-surface temperature lapse rate, and the deuterium-to-hydrogen ratio. This chapter describes the physical basis for near-IR sounding of Venus' lower atmosphere, reviews the results obtained to date, and looks briefly at the prospects for further progress in exploring an important and largely mysterious planetary regime which previously was accessible only to microwave sounding or entry probes.

I. The lower atmosphere of Venus

This section provides a brief summary of our knowledge of the lower atmosphere of Venus before the discovery of the near infrared 'windows' in 1984. At that time, only microwave observations, most significantly of deep atmosphere temperatures and water vapour amount, were thought to penetrate the thick cloud cover. Knowledge of the structure and composition of the region, in so far as it was known at all, had been obtained mainly by direct-sensing instruments on the various probes. For example, in-situ spectroscopy was carried out by instruments on some of the Russian entry probes, beginning with Venera 11 in 1978. The US Pioneer Venus (PV) entry probes of December 1978 obtained simultaneous temperature-pressure data at four sites, giving the first horizontal gradients in the deep atmosphere, and compositional and cloud microphysics profiles from a single large probe. The results of these pre-1983 investigations have been extensively published, and most of them are summarised in the Venus I book (1983).

Composition. The lower atmosphere of Venus is composed mainly of CO_2 (96.5%) and N_2 (3.5%), with small amounts of the noble gases, principally argon, and of chemically active species including H_2O, CO, OCS, SO_2, HCl, and HF. Variability in space and time is to be expected of reactive species, but the scale of the variability is virtually unknown in every case, and even the mean values are uncertain. For the best studied example, water vapour, values ranging from 20 to 25000 ppmv have been published over the last 30 years. The highest of these came from direct sampling instruments on entry probes, and were in direct conflict with ground-based microwave observations. Measurements

at frequencies near 1 cm wavelength placed upper limits on the water vapor abundance of 2-300 ppmv, assuming uniform mixing below the clouds (Janssen et al., 1973, Janssen and Klein 1981). The Venera 11,12,13 and 14 probes carried spectrophotometers which scanned the range from 0.45 to 1.2 μm with moderate spectral resolution (0.02 μm). Again using water vapor as the most important example of the results obtained from these early experiments, the probes found (Moroz, 1983, Young et al., 1984) mixing ratios close to the modern value in the lower troposphere, with larger and more ambiguous values at higher levels near the cloud decks (see section IV below).

Clouds. The Venusian clouds totally cover the planet at heights between about 45 and 70 km, with thinner hazes above and below. Instruments on the Venera 9 and 10 landers and the four PV entry probes provided simultaneous in-situ measurements of the vertical structure and particle size distributions in the clouds (see Venus I and Esposito, this book). They found that the main cloud consists of three distinct layers, separated by relatively clear regions. These layers, known as the upper (~57 to 70 km altitude), middle (~49 to 57 km), and lower (~47 to 49 km) clouds, are bounded above and below by more diffuse haze layers. Sulfuric acid (H_2SO_4) aerosols are the principal constituent of all three layers, but the particle size distributions differ from layer to layer. PV Orbiter Cloud Photopolarimeter measurements showed that the upper haze layer is composed primarily of very small "mode 1" particles, which have modal radii between 0.25 and 0.4 microns. The PV Large Probe Cloud Particle Spectrometer showed that the lower haze was also composed primarily of these particles. The upper cloud consists primarily of a second particle type, called mode 2, which has a ~1μm equivalent radius, but also includes significant numbers of mode 1 particles. A third particle type, mode 3, is the principle component of the middle and lower clouds. This consists of relatively large particles, in a distribution with a mode radius of 3.85 μm and some particles as large as 35μm equivalent radius. Mode 3 may have a crystalline component of uncertain composition. The smaller modes are found mixed in with mode 3 at all levels where the latter occurs.

The VEGA-2 lander also carried a particle size spectrometer, only the second to be deployed on Venus to date. The VEGA measurements revealed very few large particles at altitudes below 55 km, in marked contrast to the PV Large Probe, which of course entered at a different place and time. The measurements of cloud thickness by the nephelometers on the four PV probes differed by less than ~20% in the middle cloud (50-57 km), but revealed much larger differences in the particle densities within the lower cloud (47-50 km). Similar results were obtained by the nephelometers aboard Veneras 9, 10, and 11. It is now clear that the cloud opacity, the relative abundances of size modes, and possibly the modes themselves, vary considerably across the planet, and evolve in time. Studies of cloud variability using near-IR mapping are discussed in detail in section III below.

Dynamics. Before near-IR sounding became a reality, the only data on winds in the troposphere were ten profiles obtained by tracking the movements of entry probes during their descent, and surface measurements by the Venera soft landers. They show a steady decline from the high values near the cloud tops to low values near the surface (~1 ms^{-1} according to the Venera 9 and 10 landers, Avduevsky et al. 1983). Interesting vertical structure and substantial differences between locations are apparent in the profiles, but are difficult to interpret due to the small sample size.

Feature tracking in near-IR maps provides global-scale wind fields in the upper troposphere, mainly around 40-50 km where the thickest cloud layers occur. The cloud-tracked winds are generally consistent with the entry probe data in that they represent rapid zonal motion (about 50 ms^{-1} at this level, compared to nearer 100 ms^{-1} in the UV features near 70 km altitude) coupled with slower equator-to-pole drifts of a few ms^{-1}. These mean motions take place against a background of considerable meteorological activity, which is seen in the high contrast and very variable cloud morphology, as well as the winds themselves.

Tracking of entry probes provided little information about the wind profile in the lowest scale-height (~16 km) because, compared to the accuracy of the experiments, the winds there are small. Neither are there any cloud features to track at these heights, so far as we know. The situation has changed little since Schubert (1982) wrote in *Venus I*: 'The actual circulation in the lowest scale height of Venus' atmosphere is completely unknown, and the dynamics of this region, which contains 65% of the atmospheric mass, is probably crucial to the build-up of the large zonal winds at greater heights because it is likely that the atmospheric angular momentum must be transported upwards from the surface.' He calls for a network of long-lived meteorological stations on the surface of Venus, an attractive idea but one which, bearing in mind the conditions there, is well beyond current technology.

II. The Near IR Windows

A. Discovery

The first spatially-resolved near-IR images and spectra of the night side of Venus, revealing high-contrast markings at wavelengths near 1.74 and 2.3 μm, were obtained by D. Allen and co-workers in 1983. Whilst at first the observers attributed the origin of these features to scattered sunlight from the dayside, their further work indicated, and radiative transfer modelling studies later confirmed, that they are produced when thermal radiation from the hot lower atmosphere (25-40 km) escapes through differing optical depths in the planet-wide cloud layers (Figure 1). It was clear from the outset that an analysis of the spectral properties of this radiation offered a new way to probe the temperature, composition and cloud properties of the deep atmosphere.

It is surprising, perhaps, that such important behavior had not been predicted or observed earlier. In fact, the connection had not been made between three factors that contribute to the transparency of the Venus atmosphere at these wavelengths. First, concentrated sulfuric acid cloud droplets scatter almost conservatively in the near IR. Second, there are a number of spectral windows between strong CO_2 and H_2O absorption bands, where the opacity is dominated by the far wings of strong spectral lines. Finally, the CO_2 absorption in these wings is substantially less than traditional pressure-broadened line shapes predict. Thus, upwelling radiation in the near-IR windows is scattered very conservatively when it passes through the planet-wide cloud cover, and a significant fraction escapes to space. At wavelengths beyond 2.5 μm the refractive index of H_2SO_4 changes, and the cloud droplets begin to absorb strongly, blocking any further windows in the spectrum of the gaseous part of the atmosphere.

Figure 1

Fig.1 Early observed (dashed lines, Allen and Crawford, 1984) and modelled (solid line, Kamp et al., 1988) spectra for the night side of Venus.

B. Summary of Observations

Allen's pioneering observations were obtained at the Anglo-Australian Telescope (AAT) during June and July of 1983. The original detection of night-side emission from Venus was made on 15 June, 1983, as part of a near-IR survey of the solar system (Allen and Crawford, 1984). Much better imaging was possible later that year when the planet presented only a narrow crescent but was still far enough from the Sun to be observed, a condition which occurs for only about two weeks every 19 months. Time-resolved images taken during 18-23 September 1983 showed that the near-IR features moved from east to west, in the direction of the cloud-top superrotation, but with a period of 5.4±0.1 days. Images and spectra taken at wavelengths between 3 and 4.8 μm showed only the faint, nearly spatially-uniform thermal emission from the cloud tops at ~240K.

In 1990, Venus was observed from a global network of ground-based telescopes, timed to support the Galileo spacecraft, which flew past Venus on February 10, 1990. The spaceborne and ground-based observations revealed further spectral windows at 1.0, 1.10, 1.18, 1.27, and 1.31 microns, as predicted by modelling studies (§IIC). The first three of these windows sound the Venusian surface and the lowest scale height of the atmosphere, while the last two probe just above this level. The spectra at these wavelengths reveal emission contrasts associated with surface temperature variations, and have been used to

investigate the thermal structure in the lowest 6 km of the atmosphere (§V).

The motions of the near-IR features due to clouds have been measured by tracking them in ground-based and Galileo Near Infrared Mapping Spectrometer (NIMS) images (Figure 2). These data allowed wind vectors, and the approximate level of formation of the features, to be inferred. They also revealed spatial variations in the spectral properties of the cloud particles, most likely due to variable size distributions (§III).

Figure 2

Fig.2 The dark side of Venus, mapped at a wavelength of 2.3 μm in one of the most prominent of the near-IR 'windows'. It shows the highly variable nature of the opacity in the main cloud deck, illuminated from behind by thermal emision from the lower atmosphere. This view was obtained by the Near Infrared Mapping Spectrometer (NIMS) during the Galileo flyby of Venus on 10 February 1990 (Carlson et al., 1993).

Water vapor bands are detectable in the 1.10, 1.18, 1.74 and 2.3 μm windows. Near-IR spectra also provide information on the mixing ratio, horizontal distribution, and variability, of CO, HF, HCL, OCS and SO_2 below the clouds (§IV). Representative (high spatial, low spectral resolution) NIMS and (low spatial, high spectral resolution) ground-based spectra are presented in figures 3 and 4 respectively.

Figure 3

Fig.3 A representative spectrum of the dark side of Venus obtained by the NIMS instrument during the 1990 Galileo flyby (Carlson et al., 1991). The positions of some of the strongest CO_2 bands, which appear in absorption at the longer wavelengths, are indicated.

Figure 4

Fig. 4 High resolution ground-based spectra of the night side of Venus in the 2.3 μm and 1.7 μm windows, with the main absorption features identified (Bézard, 1994).

C. Interpretation and Models

Allen and Crawford (1984) speculated on the origin of the night-side NIR emission and the associated bright and dark features, but were not able to discriminate between a deep-atmosphere thermal source and a solar source. They noted that the observed high brightness temperatures at 1.74 μm (~450K) and the large absorber pathlengths (200 km atm) for the 2.33 μm CO band were consistent with a deep-atmosphere source. However, these observations alone did not completely preclude scattered sunlight as a source of the observed emission and contrasts. They also noted that even though the bright and dark NIR features superficially resembled the UV features seen at the cloud tops, their rotation periods were about 1 day longer than that of the UV features, and their contrast was much greater. These observations suggested a different level of formation for the UV and NIR features, but did not identify that level. Subsequent observations of the Venus night side taken during May 1985 confirmed the persistence of the NIR features and provided additional constraints on their origin (Allen, 1987). In particular, Allen concluded that these observations clearly precluded a solar source because (1) the brightness and contrast of the NIR features did not decrease with distance from the terminator, (2) the equivalent width of the 2.33 μm CO band did not increase with distance from the terminator, and (3) there was no detectable polarization in the night-side NIR emission. It followed that the NIR radiation must originate as thermal emission from the deep atmosphere. Similarities between spectra of bright and dark regions on the night side also suggested that the spatial contrasts were produced as thermal radiation from the deep atmosphere escapes to space through regions of the clouds that have different optical thicknesses.

These discoveries generated great interest in the planetary atmosphere community since they provided new opportunities to study the deep atmosphere of Venus. Kamp et al. (1989) were the first to use a sophisticated radiative transfer model to analyze the 1983 and 1985 AAT observations. Their modeling study confirmed that the NIR radiation could originate as thermal emission from pressure-broadened CO_2 and H_2O lines at altitudes between 25 and 55 km, and showed that ~10% horizontal variations in the cloud optical depths could produce the observed contrasts. It was found that even an approximate fit to the observations required the absorption in the far wings of CO_2 spectral lines to be much less than that predicted by the standard pressure-broadened line profiles. In fact, the near-IR windows on Venus would vanish altogether if a Lorentzian

profiles applied. Subsequent modelling work (Crisp et al, 1989; Kamp and Taylor, 1990; Bézard et al., 1990) gradually improved the fits to the measured spectra, in particular by using better spectral parameters to represent CO_2 at high temperatures and pressures. The modelling results show which regions are sounded in the various windows; a summary is given in Table 1. It can be seen that in general the windows probe deeper as the wavelength decreases, essentially because the molecular bands get weaker and the very strong CO_2 bands get further apart, so that their far wings absorb less.

Window Region (microns)	Approximate Depth Probed
1.01	Surface (>90%)
1.10	Surface (~60%) plus 0 to 15 km
1.18	surface (~40%) plus 0 to 15 km
1.27	15 to 30 km
1.31	30 to 50 km
1.74	15 to 30 km
2.3	45 to 26 km

Table 1. A list of the principal near-IR windows observed on Venus, and estimates of the approximate height ranges probed. These are fairly uncertain, especially the contribution from the atmosphere in the three shortest-wavelength windows.

The radiative transfer models have been used to interpret ground-based and spacecraft observations of near-IR spectra. The key features which need to be represented are firstly, the very high single-scattering albedo of sulphuric acid droplets at wavelengths short of 2.5 μm, and secondly, the strongly sub-Lorentzian nature of the spectral line shapes for CO_2 under the conditions found on Venus (see e.g. Brodbeck et al., 1991). The former ensures that, although photons emitted from gases in the deep atmosphere must encounter many particles in their path through the cloud layers to space, these encounters predominantly take the form of conservative scattering events and there is relatively little absorption. The fact that the CO_2 lines do not have strong wings means that the continuum absorption between the numerous bands is much weaker than a calculation based on the Lorentz pressure-broadened line shape would predict. Indeed, no complete theory for the line shape exists which predicts from first principles the small absorption in the far wings that is observed, and it is difficult to obtain the combination of high pressures and long path lengths required to study it in the laboratory. The results from Venus therefore contribute to our understanding of the forces present during the collisions of individual molecules under conditions of high temperature and pressure.

D. The leaking 'Greenhouse'

The near-IR windows radiate energy from the surface and lower atmosphere directly to space, and are therefore a new factor in the debate about how the high surface temperature is maintained.

It was confirmed at the time of Pioneer Venus (Tomasko et al., 1980) that the lower atmosphere of Venus is heated primarily by solar radiation propagating downwards through the clouds. The energy balance of the region depends on the subsequent removal of the energy so deposited, eventually by re-emission to space in the infrared. The high surface temperature is a conseqence of the fact that the loss process is quite inefficient overall, due to the high optical thickness of the overlying atmosphere at most wavelengths. The energy deposited in the lower atmosphere, mostly at low and mid-latitudes, is transported horizontally and vertically by advection and eventually radiated from the middle atmosphere, mostly at levels near the cloud tops (see the review by Crisp and Titov, this book, for a full discussion of the energy budget of Venus' atmosphere).

This convective 'heat engine' is bypassed to some extent by the flux directly to space in the near-IR windows. However, the windows occupy only a small fraction of the total spectrum, and fall at wavelengths where the Planck function has a small value compared to the mid-IR, even when the relatively high temperatures of the emitting layers are taken into account. The net effect, integrated over wavelength, is that the atmosphere below about 60 km radiates very little energy directly to space. It can be estimated from the information in figure 1, for example, that the integrated flux escaping from Venus via the near-IR windows is only about 0.05% of the total, enough to lower the equilibrium temperature of the surface of Venus by less than 1K.

III. High Spatial Resolution Near-IR Mapping of the Clouds Structure

Remote sensing in the near-IR windows probes the properties of the lower cloud layers on Venus. UV and thermal IR wavelengths do not penetrate this region, so except for isolated sampling by entry probes, there was very little data on the main cloud deck and its variability until the near-IR approach was developed. (The PV Orbiter Infrared Radiometer had a 0.4 to 4.0 μm channel, for measuring the reflected solar flux, and a narrow channel centered at 2.0 μm in a strong CO_2 band, for the detection of high clouds, but, although the former collected the flux from the near-IR windows, this is such a small part of the total that no spatially-variable features were detected). In fact, at any given point in time the intensity emanating from Venus at wavelengths within the spectral windows varies strongly with location on the planet. The net optical thickness of the cloud deck is therefore also highly variable in space and time. This implies that the lower atmosphere is very active meteorologically, one of the most exciting, and in some ways perplexing, consequences of the discovery of the properties of the near-IR windows, and one which promises much interesting exploitation in the future.

Most of the structure seen in the ground-based and NIMS images is believed to be in the main cloud deck at around 50 km altitude, which contains most of the cloud mass, i.e. well above the atmospheric layers which emit most of the near-IR

flux. In other words, we are seeing the cloud deck as a cold 'screen', back-lit by the glow from the hot atmosphere below. The remarkable variability of the cloud opacity in a single map, and the evolution with time of the features seen in successive maps, suggests high winds and vigorous convective and wave activity below the tropopause on Venus. Various features sometimes described as bars, bands, and ovals have been seen in the ground-based data, and there is a suggestion of a linear feature in the NIMS data at 45°N (see fig. 5 of Carlson et al., 1991). However, in general the cloud morphology is sufficiently complex (c.f. figure 2), and its origins sufficiently obscure, to discourage attempts to describe the meteorological regime at these levels on Venus in more specific terms at present.

The best spatial resolution obtained in near-IR mapping of Venus was by the Galileo NIMS instrument, which achieved about 25 km during closest approach on 10 February 1990. These high-resolution maps showed intensity variations of about a factor 20 between the brightest and the darkest features in the 2.3 μm window. Carlson et al. (1991) examined the wavelength dependence of the cloud opacity in different regions of the disk, and found an asymmetry in the cloud types seen in the two hemispheres. Carlson et al. (1993) refined the analysis, and found 5 distinct cloud types altogether, which they interpreted as regions of distinct mixes of Mode 2' and 3 particles.

Grinspoon et al. (1993) analysed the global contrasts between NIMS observations in the 1.7, 2.3 and 3.75 μm windows, and provided more stringent constraints on the amplitude and vertical distribution of the optical depth anomalies. They found that these variations were largely confined to altitudes between 48 and 50 km, in the lower cloud, and were mainly attributable to 'mode 3' particles with an effective mean radius (r_{eff}) of 3.65 μm. In the upper cloud they found a best fit with ~85% of Mode 2 (r_{eff} = 1 μm) and ~15% of Mode 1 (r_{eff} = 0.3 μm) particles.

Since the Galileo encounter with Venus lasted only one or two days, the NIMS observations give no information about the longer-term evolution of global structure in the middle and lower clouds. They have been augmented, therefore, using observations of the night side in the near-IR windows. Ground-based observations taken between 1988 and 1994 revealed a long-lived (>6 weeks), large-scale (zonal wavenumber 1), opaque, cloud feature at low latitudes (<40°), that extended about half-way around the planet (Crisp et al., 1989, 1991b). This feature had a rotation period of 5.5+0.15 days, comparable to that of the middle cloud region. Its maximum optical thickness could not be determined precisely, because little or no near-IR radiation escapes through it. Ground-based observations taken in January and February of 1990 show that the most transparent part of this cloud covered the night side on 10 February, when the Galileo NIMS observations were taken.

Mid-latitudes (40-60°) are usually occupied by bright zonal bands that appear to rotate with the large-scale, low-latitude feature in the middle clouds. These long-lived, partial

clearings in the middle cloud might explain the greater IR cooling detected near the cloud base by the PV North Probe Net Flux Radiometer (Revercomb et al. 1985). This cooling was originally attributed to meridional water vapor gradients, which now seem precluded by the near-IR observations (Crisp et al. 1991; Drossart et al. 1993).

The highest observable latitudes (>60°) are almost always dark and featureless in the near-IR, indicating relatively high cloud opacity. These dark clouds are at the same latitudes as the 'cold collar' detected by the Pioneer Venus OIR (Taylor et al., 1980) and ground-based mid-IR observers (Diner et al, 1976).

IV. Composition Measurements

A. Water vapor and D/H ratio

Water vapor measurements acquired by entry probes at altitudes below the clouds of Venus have produced conflicting results. The gas chromatographs aboard the Pioneer and Venera 14 probes indicated concentrations larger than 1000 ppmv near 40 km, while the PV mass spectrometer first reported a constant water concentration around 100 ppmv between 10 and 25 km, decreasing down to ~20 ppmv at the surface (Hunten et al. 1989). In a more recent reanalysis of these data, Donahue and Hodges (1992) derived an H_2O abundance close to 70 ppmv in the 10-25 km range, still sharply decreasing at lower altitudes. The scanning spectrophotometers on board the Venera 11/12 probes also indicated a strong decrease of the water abundance from ~150 ppmv at 42 km to ~20 ppmv near the surface. These results were based mainly on the analysis of the 0.94μm H_2O band. However, Young et al. (1984) pointed out that the data from the 1.13μm water vapor band could be interpreted with a constant H_2O mixing ratio of 20-30 ppmv below the clouds, while the measurements at 0.94μm could be affected by an additional absorber.

More recent spectroscopic investigations of the nightside near-IR emission have contributed significantly to this issue. Water vapor exhibits significant absorption in the windows centered at 2.3, 1.74, 1.18 and 1.10 μm. Because these windows probe different atmospheric regions in Venus' deep atmosphere, vertically-resolved information can be retrieved on the H_2O concentration profile. The observed emission originates from deeper layers as wavelength decreases: the 2.3-2.5 μm window senses a region extending roughly from 26 to 45 km. the 1.7 micron emission originates between 15 and 30 km, while the 1.18 micron originates from the 5-15 km range. Information on the horizontal variability of the water vapor profile is also available, from spectral imaging of the night side from ground-based telescopes or, with much higher spatial resolution, from the Galileo spacecraft.

Kamp et al. (1988) and Kamp and Taylor (1990) analysed the low-resolution ($\lambda/\Delta\lambda$ = 100) 2.3- and 1.7μm spectra of Allen (1987) using radiative transfer models. The best model fits using a 'sub-Lorentzian' line shape, in which the line shape factor was

a free parameter, suggested H_2O mixing ratios about 4 times less than the PV results, or about 25 ppmv. However, even the best calculated spectra did not match the observed spectra everywhere, mainly because the HITRAN database they used for CO_2 was tested under terrestrial conditions, and proved inadequate to model the high temperature and pressure conditions on Venus.

In 1990, Bézard et al. published the first high-resolution ($\lambda/\Delta\lambda$ up to 20000) spectra of the 2.3 and 1.7 μm windows recorded at the Canada-France-Hawaii Telescope (CFHT). Figure 4 shows an example covering the 2.3 μm window, in which features due to CO, COS, SO_2, CO_2, H_2O, HDO, and HF are clearly seen as distinct spectral features. Bézard et al. obtained a satisfactory fit to the observations by using a more complete description of the CO_2 spectrum than before, and including an additional continuum opacity, likely to be due to far wings of strong CO_2 bands lying outside the windows. A sub-cloud H_2O abundance around 40 ppmv was derived by fitting the H_2O absorption lines. More recently, de Bergh et al. (1995) presented high-resolution spectra of the 2.3, 1.74, and 1.18 μm windows recorded in June 1991 at the CFHT over a region centered at 15°S latitude on the night side. All three windows were best fitted with a 30±10 ppmv (±15 ppmv at 1.18 μm) mixing ratio, suggesting that the H_2O profile is essentially constant from the cloud decks to the lowest scale height of the atmosphere. No measurable horizontal variation in the H_2O abundance could be found in a set of 2.3μm spectra recorded at various locations on the night side, from 15°S to 30°N latitude.

de Bergh et al.(1991) took advantage of the presence of both H_2O and HDO lines in the 2.3 μm window to obtain the relative abundances of both species beneath the clouds. They obtained a value for the deuterium-to-hydrogen (D/H) ratio equal to 120±40 times the telluric value (Figure 5). Such a large proportion§ of deuterium in Venus relative to Earth was first proposed as a result of the analysis of Pioneer Venus orbiter and probe data (discussed by Donahue et al., this book), and more recently confirmed by airborne observations of H_2O and HDO lines near 2.6 micron probing the Venus cloud tops (Bjoraker et al., 1992). The enrichment probably results from photodissociation of normal and heavy water molecules in the high atmosphere, and subsequent mass-selective hydrogen escape. Whether it constitutes evidence for a lost primordial ocean, or just the steady state between loss by escape and supply by comets or volcanic outgassing, remains uncertain due to limitations in our knowledge of the escape flux of hydrogen, the cometary influx of water, and the outgassing rate of water from the surface.

Figure 5

Fig. 5 Ground based spectra of Venus showing the sensitivity to the mixing ratio of HDO. The best fit between computed and

measured spectra is for 1.30 ppmv of HDO and 34 ppmv of H_2O. After de Bergh et al. (1991).

On 29 January, 1990, Bell et al. (1991) used the Cooled Grating Array Spectrograph at the NASA Infrared Telescope Facility to record moderate-resolution ($\lambda/\Delta\lambda = 1500$) spectra of dark and bright near-IR features on the Venusian night side. These spectra indicated very different H_2O abundances according to the brightness of the region (figure 6). Mixing ratios near 40 ppmv were derived from the dark spot spectra, while the spectra of an anomalously bright spot indicated H_2O mixing ratios as high as 200 ppmv. The experimenters suggested that the bright near-IR emission and the factor of 5 increase in H_2O mixing ratios might be due to the subsidence and evaporation of a significant faction of the H_2SO_4 droplets in the middle and lower cloud decks, with subsequent thermal dissociation of the H_2SO_4 vapor into H_2O and SO_3. About 10 days after these observations, on 9 February, 1990, narrow-band filter images taken within the 2.3 micron window with the Palomar 5m Prime Focus near-IR Camera observed the bright spot seen by Bell et al., but, like all subsequent measurements, found no significant horizontal variation in H_2O.

Figure 6

Fig.6 Spectra of hot and cold spots on Venus, with model fits (Bell et al., 1991). The amount of water vapour required to achieve a good fit was substantially different for the two regions.

An analysis of 2.3 and 1.27 μm spectra with resolutions up to ~2000 recorded in 1990 at the Anglo-Australian Telescope (AAT) indicated H_2O mixing ratios of 40±20 ppmv (Crisp et al. 1991). Images of the night side using a set of narrow filters within the 2.3 μm window indicated no significant horizontal variation in H_2O. More recently, Pollack et al. (1993) presented a more complete analysis of AAT spectra including all windows from 1.1 to 2.3 μm. They also made use of Bézard et al.'s (1990) CFHT spectra at higher spectral resolution to better constrain the atmospheric model. They deduced that the H_2O mixing ratio has a constant value of 30±10 ppmv in the altitude range from 10 to 40 km.

A preliminary analysis of the Galileo NIMS 2.3 and 1.7 μm window spectra (Carlson et al. 1991) yielded H_2O mixing ratios around 25 and 50 ppmv respectively, but with a larger uncertainty than the ground-based data due to the limited spectral resolution (0.026 μm). The data at 1.18 μm were later analysed to search for possible horizontal variations of water vapor in the 5-15 km range (Drossart et al. 1993). A best fit to the spectrum was

obtained with a water vapor abundance similar to that inferred from ground-based observations (30±15 ppmv), and no horizontal variation in excess of 20% was found in the dataset, which covered a band of longitudes between latitudes of 60°S and 64°N at a spatial resolution up to 25 km.

Measurements acquired by the PV Large Probe Neutral Mass Spectrometer (LNMS) indicate that the water mixing ratios decrease substantially between 10 km and the surface (Donahue and Hodges, 1992), a result which has important implications for the presence of sources or sinks of water near the surface. The vertical distribution of H_2O in this region of the atmosphere cannot be retrieved from individual near-IR spectra because the contribution function is too broad (~20 km, Pollack et al. 1993). However, it can be derived from spatially resolved spectra, because the column-integrated H_2O optical depths in adjacent high and low surface elevation regions can be subtracted to yield the temperature lapse rate and the H_2O column abundance between the two levels. This experiment was attempted using spatially-resolved low spectral resolution ($\lambda/\Delta\lambda$~400) spectra of the night side collected with the Infrared Imaging Spectrometer on the AAT in July 1991 (Meadows and Crisp, 1996). The best fit to the data was obtained with a water vapor mixing ratio of ~20 ppmv at the cloud base, increasing to 45(+10,-15) ppmv at the 10 bar level then remaining constant at 45 ppmv down to the surface. These results appear to preclude any large decrease in the H_2O mixing ratios near the surface, contrary to the PV LNMS observations.

The lack of evidence of any significant concentration gradient below the 10 bar level (~30 km) also contrasts with the predictions of thermochemical calculations (Lewis and Grinspoon, 1990). In their model, H_2O reacted with CO_2 in the lower atmosphere to form carbonic acid gas (H_2CO_3), yielding an H_2O vertical profile roughly consistent with the Venera spectrophotometric measurements at 0.94 μm. However, the water profiles from nightside spectroscopic observations indicate that this conversion to H_2CO_3 probably does not occur. The low abundance of H_2O also has some important implications for the stability of hydrated silicates on the surface of Venus, as discussed by Fegley et al. (this book).

In summary, the net evidence based on remote sensing observations suggests that the atmosphere of Venus is extremely dry, on the average at least, much dryer than indicated by most of the *in situ* probe measurements. The water vapor mixing ratio apperars to be approximately constant both horizontally and vertically, in the lowest 30 km at least, with a value between 20 and 50 ppmv.

B. Carbon Monoxide

The (2-0) band of CO, visible in the early observations of Allen and Crawford (1984), is a prominent feature located around 2.35 μm near the center of the 2.3μm window. First analyses of these low resolution observations (Kamp et al. 1988; Kamp and Taylor

1990) seemed to indicate CO abundances considerably lower than those measured by the PV gas chromatograph (which were 30 ppmv at 52 and 42 km; 20 ppmv at 22 km, according to Oyama et al. 1980). However, as for water vapor, these values had uncertainties originating in the poor state of the spectral line database on weak CO_2 bands under Venusian conditions. Using an improved representation of the CO_2 opacity, Bézard et al. (1991) fitted their high resolution CFHT spectra with a CO profile around 1.5 time the PV profile. A more recent attempt to reproduce these observations using a still more sophisticated database for CO_2 led to CO abundances similar to the PV measurements (Bézard , 1994).

Pollack et al. (1993) analysed the AAT spectra of Crisp et al. (1991), deriving a CO mixing ratio equal to 23±5 ppmv at 36 km. They were also able to infer the CO vertical gradient around this level by simultaneously fitting the P- and R-branches of the CO band. They found that the concentration declines by a factor of 1.5 between 32 and 40 km, a trend in agreement with the PV profile. Further implications of these findings are discussed in Section D below.

A preliminary modelling of the CO absorption feature in the Galileo NIMS spectra of the 2.3 μm window estimated a mixing ratio around 50 ppmv near 30 km (Carlson et al. 1991). A more comprehensive analysis of the NIMS spectra by Collard et al. (1993) reduced this to around 30 ppmv, and detected a definite latitudinal trend (fig.7). Investigating the whole set of ~500 spectra spanning latitudes between 60°S and 70°N, they found that the depth of the CO absorption band was significantly larger northward of ~47°N. This corresponded to a CO mixing ratio which was 20-50% higher in the northern polar region than the value of 1.17±0.1 times the PV profile found at lower latitudes in either hemisphere. It was not possible to say whether a similar enhancement existed in the southern polar region, because the trajectory of Galileo favoured observations of the northern hemisphere of Venus and high-latitude data was not obtained in the south. High latitudes are also inaccessible to Earth-based observers due to the small inclination of Venus' axis of rotation. Only new observations from future high-inclination spacecraft can confirm the existence of the northern polar CO enhancement, see if the equivalent is present in the southern hemisphere, and observe how they vary with time. It should then be possible to say how the anomaly arises. The various possibilities include localised volcanic activity, or (more probably) transport of CO from the upper atmosphere in the polar vortices, with major implications for the general circulation of the whole atmosphere (Taylor, 1995).

Figure 7

Figure 7. The distribution of carbon monoxide with latitude, inferred from the 0-2 band observed near 2.3 μm by Galileo-NIMS

(after Collard et al., 1993 and Taylor, 1995). The abundance scale refers to the mean mixing ratio in a broad layer about 20 km thick centred on about 40 km altitude.

C. Hydrogen halides

HCl and HF were detected originally at the cloud tops of Venus from high resolution near infrared spectroscopy of reflected light from the day side. Connes et al. (1967) derived mixing ratios of 0.6 ± 0.1 ppmv for HCl and $5.0^{+5.0}_{-2.5}$ ppbv for HF. More recent observations near 3.6 μm by de Bergh et al. (1989) indicated ~0.4 ppmv HCl near 70 km altitude. These abundances were below the sensitivity levels of the instruments on the Pioneer and Venera probes.

Spectroscopic analyses of the nightside near-IR emission provided the first measurements of the HCl and HF mixing ratios below the clouds. Bézard et al. (1990) detected a few HF lines in their high resolution CFHT spectra at 2.3μm, and several lines from the ^{35}Cl and ^{37}Cl isotopes of HCl in the 1.7μm window. They derived mixing ratios of ~0.5 ppmv for HCl (pertaining to the 15-30 km altitude range), and ~4.5 ppbv for HF in the 30-40 km region. Pollack et al. (1993) inferred concentrations of 0.48 ± 0.12 ppmv for HCl, and between 1 and 5 ppbv for HF, using lower resolution AAT spectra.

The HCl and HF mixing ratios below the clouds thus appear similar to those measured at the cloud tops 20 years before. This constancy suggests that the observed abundances are equilibrium values rather than controlled by episodic volcanism. Fegley and Treiman (1992) emphasised that these reactive gases are likely to be in equilibrium with the surface mineralogy, and described different possible assemblages, involving alkaline rocks, capable of buffering their abundances.

D. Sulfur-bearing compounds

Carbonyl sulfide (OCS) was first unambiguously detected by Bézard et al.(1990) in their 2.3μm CFHT spectra of the night side of Venus. They derived a mixing ratio of about 0.25 ppmv under the assumption that it was uniformly mixed below the clouds. Pollack et al. (1993) showed that it is possible to infer the vertical gradient of the OCS concentration from the shape of the absorption feature at the OCS band head near 2.43 μm (Figure 8). Fitting Crisp et al.'s (1991) AAT spectra, they found that the OCS mixing ratio increases sharply with decreasing altitude. A mixing ratio equal to 4.4 ± 1 ppmv was derived for the 33-km level, increasing to some 20-40 ppmv at 28 km. A re-analysis of the high-resolution CFHT spectra, allowing for a vertical gradient in the OCS profile, gave consistent results: a mixing ratio of 0.35 ± 0.10 ppmv at 38 km from the absorption at the band head at 2.43μm, and an increase to 10-20 ppmv at and below 30 km to reproduce the low-wavelength wing of the band (Bézard , 1994).

Figure 8

Fig.8 (Left) Observed and measured spectra in the 2.3 μm window showing features due to carbonyl sulfide (OCS). (Right) The range of OCS vertical profiles which provide a possible fit to the spectra. From Pollack et al., 1993.

As noted by Pollack et al.(1993), there is some evidence that the decrease in OCS mixing ratio by about 10 ppmv between 30 and 38 km is matched by a increase in CO of about the same amount. The retrieved CO and OCS profiles are in good agreement with recent chemical kinetic modelling by Krasnopolsky and Pollack (1994) in which OCS is destroyed by reaction with SO_3 to yield CO above ~33 km. If the OCS mixing ratio is constant between ~28 km and the surface, this would be consistent with the equilibrium abundance calculated from pyrite chemical weathering, suggesting that iron sulfides are stable on Venus' surface (Fegley and Treiman 1992).

The sulfur dioxide (SO_2) abundance beneath the cloud decks was first measured by the gas chromatographs carried by the PV and Venera 11/12 probes in 1978. The PV data yielded 185±43 ppmv at 22 km altitude, while a mixing ratio of 130±35 ppmv was derived below 42 km from the Venera measurements (Von Zahn et al. 1983). More recently, an analysis of the ultraviolet spectra recorded by the VEGA 1 and 2 probes in June 1985 yielded a SO_2 profile strongly decreasing downwards below the cloud decks and reaching 20-25 ppmv at 12 km (Bertaux et al., 1996; see also Fegley et al., this book).

Absorption by the weak $3\nu_3$ band of SO_2 near 2.45 μm was detected in CFHT spectra of the night side by Bézard et al. (1993). They derived an average mixing ratio of 130±40 ppmv over the 35-45 km region (Figure 9). No spatial variation was detected over a set of 4 spectra recorded in 1989 and 1991 at different latitudes between 15°S and 30°N. Consistent with this, Pollack et al. (1993) derived a SO_2 mixing ratio of 180±70 ppmv using AAT spectra recorded in February 1990.

Figure 9

Fig.9 Observed and synthetic spectra for a region near 2.45 μm containing the $3\nu_3$ band of SO_2, showing the best fit value of 130 ppmv and the effect on the spectrum of varying this from 0 to 500 ppmv. From Bézard et al. (1993).

Thus, within the uncertainties, the deep-atmosphere SO_2 mixing ratios derived from nightside spectra are the same as those measured by the Venera, PV and probes from 1978 to 1985. This stability contrasts with the apparent massive decrease observed

at the cloud tops from UV spectroscopy over the period 1978-1988 (Esposito et al., this book). Since it is not matched by changes in the lower atmosphere, this decrease may indicate long-term changes in the circulation of the upper atmosphere, affecting the composition there, rather than a manifestation of a major volcanic eruption as originally proposed by Esposito (1984). The constant values observed below the cloud decks are consistent with the extremely low reaction rates of SO_2 with calcium-bearing minerals at the surface, which imply a removal time constant larger than 10^6 years (Fegley and Treiman 1992).

E. Summary of Current Knowledge of the Composition

Table 2 provides current best estimates, with realistic uncertainties, of the mean mixing ratios of those gases which have been identified to date in nightside spectra of Venus.

V. Dynamics

At levels within the clouds (47-70 km), the Venusian atmosphere rotates westward fifty to sixty times faster than the solid body of the planet, driven by mechanisms which remain mysterious after more than two decades of detailed study (Gierasch et al., this book). A comprehensive description of the winds at the cloud-top levels where this 'super-rotation' is most intense has been derived by tracking features in Mariner 10, PV and Galileo UV images, but they contribute little insight into the processes that must transport momentum from the planet's surface to these altitudes.

The winds below the cloud tops were obtained by tracking the PV, Venera, and VEGA entry probes as they descended through the atmosphere. These measurements show that the winds blow from east to west at all levels, with amplitudes that decrease almost monotonically with altitude. The descent probe measurements are again too limited in spatial and temporal sampling to discriminate between atmospheric waves and the time- and space-averaged motions. They also lack the accuracy needed ($\pm$1 m/s) to describe the much smaller zonal winds in the lowest scale height (~ 16 km), or the meridional winds at any level, well enough to understand the role which momentum transport by the meridional circulation and vertically-propagating waves may play in the maintenance of the superrotation.

The deep-atmosphere probe afforded by near-IR spectroscopy offers the possibility of a more comprehensive global description of dynamics in the middle and lower cloud regions to complement the probe and balloon data. Winds derived from near-IR feature rotation periods have been acquired during the each of the Venus inferior conjunctions since the discovery of the features in 1983. Allen and Crawford (1984) found that the night-side near-IR features at wavelengths near 1.74 and 2.3 μm moved in the same direction as the cloud-top super-rotation, but with a somewhat longer period (~5.5 days). Subsequently, simulations with radiative transfer models showed that these features are associated with optical depth variations within the middle (49-57 km) and lower (47-49 km) clouds. During the

observing campaign conducted to support the Galileo flyby before and after the January 1990 inferior conjunction, the markings were tracked to produce a global, 2-dimensional description of horizontal winds in both of these cloud decks (Crisp et al. 1991b). The middle cloud was dominated by a long-lived

Gas	Mixing Ratio (ppmv)	Altitude (km)	Reference
H_2O	30±10	26-45	(1,2)
	30±10	15-30	(1,2)
	30±15	0-15	(1,3)
D/H	120±40 ⊕	26-45	(4)
CO	23±7	30	(2,5)
	29±7	40	(2,5)
HF	0.005±0.002	30-40	(5)
HCl	0.5±0.15	15-30	(5)
OCS	14±6	30	(2,5)
	0.35±0.1	38	(2,5)
SO_2	130±40	35-45	(6)

TABLE 2. Recommended values for mixing ratios of minor gases measured from spectroscopic investigations of the nightside emission. The references are: (1): de Bergh et al. (1995), (2): Pollack et al. (1993), (3): Meadows and Crisp (1996), (4): de Bergh et al. (1991), (5): Bézard (1994), (6): Bézard et al. (1993). The symbol ⊕ refers to the terrestrial value.

wavenumber 1 feature, with a rotation period of 5.5 + 0.15 days, indicating equatorial velocities near 80 m/s. The lower cloud was characterised by short-lived small-scale features that had rotation periods of 7.4 ± 1 days. The meridional structure of the zonal motions of both cloud decks was indistinguishable from solid-body rotation at latitudes equatorward of 60-degrees. No systematic north-south motions were observed in the 6-week-long ground-based feature tracking experiments, indicating an upper limit of about 0.5 m s^{-1} on mean meridional winds in the middle cloud, and about 7 m s^{-1} for those in the lower cloud.

The two Galileo NIMS images acquired during the February 10, 1990 flyby have also been used to infer wind velocities in the northern hemisphere (Carlson et al., 1991). These observations provide much more stringent constraints on small near-IR feature displacements since their resolution is about a factor of 10 better than that of the best ground-based results. In contrast to the (almost contemporaneous) ground-based observations, which indicate solid-body rotation, the NIMS results appear to show an increase in the westward wind velocity with latitude. Crisp et al. (1991b) proposed that this apparent increase may be a consequence of the meridional variations in the altitude of near-IR feature formation, rather than an actual meridional wind gradient. At the time of the NIMS observations, the lower latitudes were dominated by features in the more slowly-moving lower cloud layer, while the high latitude regions were dominated by features in the faster-moving upper cloud region. The NIMS observations also revealed slow poleward motions in both hemispheres, of the order of a few m s^{-1}, but with error bars of the same magnitude.

VI. The Surface and the Near-Surface Atmosphere

In the very short wavelength windows, at 1.0, 1.1, and 1.18 microns, the total column opacity of the atmosphere is low enough that thermal emission from the surface can be detected. The surface contributes ~60% of the emission in the 1.18-micron and ~40% in the 1.1-micron windows; and more than 95% within the 1.0-micron window (Meadows and Crisp, 1996). Maps made at these wavelengths reveal the topography with fairly high contrast, since the higher features are cooler and the rate of change of the Planck function with temperature is large at 1μm and 730K. For example, the highest feature, Maxwell Montes, which was also the first detected in this way (Carlson et al., 1991), is about 10 km higher, and therefore about 80K cooler, than its surroundings. The radiance contrast at 1μm, assuming the same emissivity, is more than an order of magnitude. Surface features such as Beta Regio, Phoebe Regio, and Ulfrum Mons are 20 to 50% darker than the surrounding plains because they are up to 45 K cooler. Contrasts much smaller than this are detectable in NIMS images of Venus, and the cooler features observed in the near-visible IR windows correlate well with regions of elevated topography found in maps made by the Pioneer Venus and Magellan radars.

Surface features have since been detected in ground-based near-IR observations with a maximum spatial resolution of about 100

km horizontally, but as small as 1 km vertically (Meadows et al. 1992; Lecacheux et al. 1993, Meadows, 1994; Meadows and Crisp, 1996). Meadows (1994) and Meadows and Crisp (1996) used AAT/IRIS image cubes taken in July 1991 to provide new constraints on the atmospheric temperature lapse rates near the surface. Their analysis used simultaneous observations taken within the 1.31 and 1.18 μm windows to correct for intensity differences associated with horizontal variations in the cloud optical depths. Synthetic spectra were calculated for a range of topographic elevations and combined with PV altimetry data to produce spatially-resolved maps of the NIR thermal emission from the night side. Comparisons between these synthetic radiance maps and the IRIS observations indicated temperature lapse rates between -7 and -7.5 K km^{-1} in the lowest ~6 km of the atmosphere, significantly smaller than the values of -8 to -8.5 K km^{-1} inferred from earlier measurements and greenhouse models.

VII. Major Open Questions and Future Work

An obvious goal is for future spacecraft missions to Venus is to exploit the remarkable properties of the near-IR windows to study the meteorology of the deep atmosphere at much higher spatial and time resolution than is possible from the Earth. Instruments on high-inclination orbiting spacecraft could provide good coverage of the polar regions, where the atmospheric behaviour is known to be markedly different from the lower-latitude regions accessible to Earth-based observers, and seems to have a key role in the atmospheric general circulation on Venus. In particular, it is fascinating to imagine how the polar vortices might appear in movies constructed from near-IR images. Investigations of the deep structure around the poles may shed light on the complex dipole and cold polar collar features discovered by Pioneer Venus (Taylor et al., 1980).

Insight into the zonal, meridional and vertical motions at various levels, and meteorological activity on Venus in general, can be obtained from studies of the character and morphology of the features at different near-IR window wavelengths, particularly if high spatial resolution and long-term coverage are available. The behaviour of the major features seen in ground-based images suggests planetary-scale waves, while the general appearance of the clouds and the large opacity contrasts indicate large-scale convective cells at many locations (c.f. Figure 2). The middle latitudes of both hemispheres are often occupied by bright, quasi-zonal bands (Crisp et al., 1991b) which may be evidence for large-scale subsidence. If this is the case, they may reveal under closer study from spacecraft the poleward extent of the low-latitude Hadley cell, with important implications for models of the general circulation and processes affecting the maintenance of the cloud-level super-rotation.

In principle, it should be possible to derive a more global description of the near-surface winds from the temperature and pressure fields, but this is not currently possible because, despite various attempts, these fields are as poorly constrained as the winds themselves. The Magellan orbiter obtained passive microwave observations of the surface, but these could not yield

a global description of the temperature field because of uncertainties in the absolute radiometric calibration of its antenna (Pettengill et al. 1992). Both approaches offer the possibility, in the future, for temperature mapping of the surface and lower troposphere with sufficient precision to shed light on the circulation at these depths.

High-resolution near-IR spectroscopy can be used to obtain information on the species known or suspected to be variable in space and/or time, for example carbon monoxide, sulfur dioxide, and water vapor. A detailed study of these will lead to a better understanding of the coupling of dynamics and chemistry in the cloud layers and near the surface. Monitoring trace gases like OCS, SO_2, H_2O, or CH_4 at 2.3 μm is also a way of looking for volcanic activity. Again, these measurements would be most effectively conducted from an orbiting spacecraft.

VIII. References

Allen, D. and Crawford, J., 1984. Discovery of cloud structure on the dark side of Venus. *Nature*, **307**, 222-224.

Allen, D., 1987. The dark side of Venus, Icarus **69,** 221-229.

Avduevskiy, V.S., et al., 1983. Structure and Parameters of the Venus Atmosphere According to Venera Probe Data. In *Venus* (eds Hunten, D.M., Colin, L., Donahue, T.M. and Moroz, V.I.) 280-298.

Baker, N.L., and Leovy, C.B., 1987. Zonal winds near Venus' cloud top level: a model study of the interaction between the zonal mean circulation and the semidiurnal tide. Icarus, **69,** 202-220.

Bell, J. III, Crisp,D., Lucey, P.G., Ozoroski, T.A., Sinton, W.M., Willis, S.C., and Campbell, B.A., 1991. Spectroscopic observations of bright and dark emission features on the night side of Venus. *Science* , **252**, 1293-1296.

Belton, M.J.S., et al., 1976. Space-time relationships in UV markings on Venus. J. Atmos. Sci., **33,** 1383-1393.

Belton, M.J.S., et al., 1991. Imaging of Venus from Galileo: Early results and camera performance. *Science* , **253**, 1531-1538.

Bertaux J.L., Widemann,T., Hauchecorne, A., Moroz, V.I., and Ekonomov, A.P., 1996. Vega-1 and Vega-2 entry probes: an investigation of local UV absorption in the atmosphere of Venus. *J. Geophys. Res.*, submitted.

Bézard, B., de Bergh, C., Crisp. D., and Maillard, J.P., 1990. The deep atmosphere of Venus revealed by high-resolution nightside spectra. *Nature*, **345**, 508-511.

Bézard, B., de Bergh, C., Fegley, B., Maillard, J.P., Crisp, D., Owen, T.C., Pollack, J.B., Grinspoon, D., 1993. The abundance

of sulphur dioxide below the clouds of Venus. Geophysical Research Letters, **20,** 15, 1587-1590.

B. Bézard. The deep atmosphere of Venus probed by near-infrared spectroscopy of the night side. Communication at the 30th COSPAR scientific assembly (session C3.1), Hamburgh, Germany 11-21 July 1994.

Bjoraker, G.L., H.P. Larson, M.J. Mumma, R. Timmermann, J.L. Montani, 1992. Airborne Observations of the Gas Composition of Venus above the Cloud Tops: Measurements of H2O, HDO, HF and the D/H and 18O/16O Isotopic ratios. B.A.A.S. **24**, 995.

Brodbeck, C., Nguyen Van-Thanh, Bouanich, J.P., Boulet, C., Jean-Louis, A., Bézard , B., and de Bergh, C., 1991. Measurements of pure CO_2 absorption at high densities near 2.3 μm. *J. Geophys. Res.*,**96,** E2, 17,497-17,500.

Carlson, R.W., K.H. Baines, Th. Encrenaz, F.W. Taylor, P.Drossart, L.W. Kamp, J.B. Pollack, E.Lellouch, A.D. Collard, S.B. Calcutt, D.Grinspoon, P.R. Weissman, W.D. Smythe, A.C. Ocampo, G.E. Danielson, F.P. Fanale, T.V. Johnson, H.H. Kieffer, Matson, D. L., McCord, T.B., and L.A. Soderblom, 1991. Galileo infrared imaging spectroscopy measurements at Venus. Science, 253:1541 -1548.

Carlson, R.W, Kamp L., Baines, K., Pollack, J.B., Grinspoon, D., Encrenaz, Th., Drossart, P., and Taylor, F.W., 1993. Distinct Venus Cloud types as Observed by the Galileo Near Infrared Mapping Spectrometer. Planetary and Space Science, **41,** 7, 477-486.

Carlson, R.W. and Taylor, F.W., 1993. The Galileo Encounter with Venus: results from the Near Infrared Mapping Spectrometer. Planetary and Space Science, **41,** 7, 475-476.

Collard, A.D., Taylor, F.W., Calcutt S.B., Carlson, R.W., Kamp L., Baines, K., Encrenaz, Th., Drossart, P., Lellouch, E., and Bézard , B., 1993. Latitudinal distribution of carbon monoxide in the deep atmosphere of Venus. *Planetary and Space Science*, **41,** 7, 487 - 494.

Connes, P., J. Connes, W.S. Benedict, and L. Kaplan, 1967. Traces of HCl and HF in the atmosphere of Venus. Astrophys. J. **147,** 1230-1237.

Counselman, C.C., et al., 1980. Zonal and meridional circulation of the lower atmosphere of Venus determined by radio interferometery. J. Geophys. Res. **85,** 8026-8030.

Crisp, D., Sinton, W.M., Hodapp, K.W., Ragent, B., Gerrault, F., Goebel, J.H., Probst, R.G., Allen, D.A., Pierce, K., and Stapelfeldt, K.R., 1989. The nature of the features on the Venus night side. *Science* , **246**, 506-509.

Crisp, D., Allen. D.A., Grinspoon, D., Pollack, J.B., 1991a. The dark side of Venus: Near infrared images and spectra from the Anglo-Australian Observatory. *Science* , **253**, 1263-1266.

Crisp, D., S.McMuldroch, S.K. Stephens, W.M. Sinton, B.Ragent, K.W. Hodapp, R.G. Probst, L.R. Doyle, D.A. Allen, and J.Elias, 1991b. Ground-based near-infrared imaging observations of Venus during the Galileo encounter. Science, **253**:1538 -1541.

de Bergh, C., Maillard, J.P., Bézard , B., Owen, T., Lutz, B.L. 1989. Ground-based high resolution spectroscopy of Venus near 3.6 microns. Bull. Amer. Astron. Soc. 21, 926.

de Bergh, C., Bézard , B., Owen, T.C., Crisp, D., Maillard, J.P., 1991. Deuterium on Venus: Observations from Earth. *Science* , **251**, 547-549.

de Bergh, C., Bézard , B., Crisp, D., Maillard, J.P., Owen, T., Pollack, J.B., Grinspoon, D., 1995. Water in the deep atmosphere of Venus from high-resolution spectra of the night side. *Adv. Space Res.*, **15,** 4, 79-88.

Diner, D.J., Westphal,J.A., and Schloerb F.P., 1976. Infrared imaging of Venus: 8-14 micrometers Icarus, **27,** 191-195.

Donahue, T.M., et al., 1982. Venus was wet: a measurement of D to H. Science **216,** 630-633.

Donahue, T.M., and Hodges Jr., R.R., 1992. The past and present water budget of Venus. J.Geophys. Res. **97,** 6083-6092.

Drossart, P., Bézard ,B., Encrenaz, Th., Lellouch,E., Roos,M., Taylor, F.W., Collard, A.D., Calcutt,S.B., Pollack, J.B., Grinspoon, D.H., Carlson,R.W., Baines, K.H., and Kamp, L.W., 1993. Search for spatial variations of the H_2O abundance in the lower atmosphere of Venus from NIMS-Galileo. Planet. Space Sci., 41(7):495 -504.

Esposito, L.W., Winick,J.R., and Stewart,A.I.F., 1979. Sulfur dioxide in the Venus atmosphere: distribution and implications. Geophys. Res. Letters **6,** 601-604.

Esposito, L.W., 1984 Sulfur dioxide: episodic injection shows evidence for active Venus volcanism. Science, **223,** 1072-1074.

Fels, S. and Lindzen, R.S., 1974. The interaction of thermally excited gravity waves with mean flows. Geophys. Fluid Dyn. **6,** 149-192.

Fegley Jr., B., and Treiman, A.H., 1992. Chemistry of atmosphere-surface interactions on Venus and Mars. In 'Venus and Mars: Atmospheres, ionospheres, and solar wind interaction', ed. J. Luhmann and P.R.O. Fegley, 70-71.

Gierasch, P.J., 1975. Meridional circulation and the maintenance of the Venus atmospheric rotation. J. Atmos. Sci. **32,** 1032-1044.

Gierasch, P.J.,1987. Waves in the atmosphere of Venus. Nature, **328,** 510-512.

Grinspoon, D.H., and Lewis, J.S., 1988. Cometary water on Venus: implications of stochastic impacts. Icarus, **74,** 21-35.

Grinspoon, D.H., Pollack,J.B., Sitton,B.R., Carlson,R.W., Kamp, L.W., Baines,K.H.,Encrenaz, Th., and Taylor,F.W., 1993. Probing Venus's cloud structure with Galileo NIMS. Planet. Space Sci., 41(7):515 -542.

Grinspoon, D.H., 1993 Implication of the high D/H ratio for the sources of water in Venus' atmosphere. Nature, **363,** 428-431.

Hunten, D.M., Donahue, T.M., Walker, J.C.G., and Kasting, J.F., 1989. Escape of atmospheres and loss of water. In 'Origin and evolution of planetary and satellite atmospheres', ed. S.K. Atreya, J.B. Pollack, and M.S. Matthews, U. Arizona Press, 386-422.

Janssen, M.A., Hills, R.E., Thornton, D.D., and Welch, W.J., 1973. Venus: new microwave measurements show no atmospheric water vapor. Science, **179,** 994-997.

Kamp, L.W., Taylor, F.W., and Calcutt, S.B., 1988. Structure of Venus' atmosphere from modelling of night side infrared spectra. *Nature,* **336,** 360-362.

Kamp, L.W. and Taylor,F.W., 1990. Radiative transfer models of the night side of Venus. *Icarus,* **86,** 510 -529.

Kawabata, K., et al., 1980. Cloud and haze properties from Pioneer Venus photopolarimetry. J. Geophys. Res. 85 8129-8140.

Kerzhanovich, V.V. and Marov,M. Ya., 1977. On the wind velocity measurements from Venera spacecraft data. Icarus **30,** 320-325.

Kerzhanovich, V.V. and Marov,M. Ya., 1982. The Atmospheric dynamics of Venus according to doppler measurements aboard the Venera automatic interplanetary stations. NASA Tech. Mem. 76818.

Knollenberg, R., Travis,L., Tomasko,M., Smith,P., Ragent,B., Esposito,L., McCleese,D., Martonchik,J., and Beer,R., 1980. The clouds of Venus: A synthesis report. J.Geophys. Res., 85(A13):8059 -8081.

Knollenberg, R.G., and Hunten,D.M. 1980. The microphysics of the clouds of Venus: Results of the Pioneer Venus particle size spectrometer experiment. J.Geophys. Res., 85(A13):8038 -8058.

Krasnopolsky, V.A., and Pollack, J.B., 1994. H_2O-H_2SO_4 system in Venus' clouds and OCS, CO, and H_2SO_4 profiles in Venus' troposphere. *Icarus,* **109,** 58-78.

Lecacheux, J. Drossart, P., Laques, P., Deladerriere, F., and Colas, F., 1993. Detection of the surface of Venus at 1.0 μm

from ground-based observations. *Planet. Space Sci.* , **41**, 543-549.

Lewis, J. and Grinspoon, D. H.,1990. Vertical distribution of water in the atmosphere of Venus: a simple thermochemical explanation. Science **249,** 1273-1275.

Linkin, V.M., Kerzhanovich, V.V., Lipatov, A.N., Shurupov, A.A., Seiff, A., Ragent, B., Young, R.E., Ingersoll, A.P., Crisp, D., Elson, L.S., Preston, R.A., and Blamont, J.E., 1986. Thermal structure of the Venus atmosphere in the middle cloud layer, Science, **231,** 1420-1422.

McElroy, M.B., Prather, M.J., and Rodriguez, J.M., 1982. Escape of Hydrogen from Venus. Science **215,** 1614-1615.

Marov, M. Ya., Lystsev, V.E., Lebedev, V.N., Lukashevich, N.L., and Shari, V..P., 1980. The structure and microphysical properties of the Venusian clouds: Venera 9, 10, and 11 data. Icarus **44,** 608-639.

Meadows, V., Crisp, D., Allen. D.A., 1992. Ground-based near-IR observations of the surface of Venus.*International Colloquium on Venus,* LPI Cont. No 789, 70-71.

Meadows, V.S., 1994. Infrared Observations with IRIS: From Planets to Galaxies, PhD. Thesis, Department of Astrophysics, University of Sydney.

Meadows. V. and D. Crisp, 'Ground-Based Near-Infrared Observations of the Venus Night Side: The Thermal Structure and Water Abundance near the Surface,' J. Geophys. Res. In Press, 1996.

Moroz, V.I., 1983. Summary of the Preliminary results of the Venera 13 and 14 Missions. In *Venus* (eds Hunten, D.M., Colin, L., Donahue, T.M. and Moroz, V.I.) 45-68.

Moshkin, B.E., Moroz,V.I., Gnedykh, V.I., Grigor'ev,A.V., Zasova, L.V., and Ekonomov,A.P., 1986. Vega 1, 2 optical spectrometry of Venus atmospheric aerosols at the 60-30 km levels: preliminary results. Sov.Astron.Lett., 12(1):36-39.

Oyama, V.I., et al., 1980. Pioneer Venus gas chromatography of the lower atmosphere of Venus. J. Geophys. Res. **85,** 7891-7902.

Pettengill, G.G., Ford, P.G., and Wilt, R.J., 1992. Venus surface radiothermal emission as observed by Magellan. J. Geophys. Res., **97,** 13091-13102.

Pollack, J.B., Toon,O.B., and Boese, R., 1980. Greenhouse models of Venus' high surface temperature, as constrained by Pioneer Venus measurements. J.Geophys. Res., 85:8223-8231.

Pollack, J.B., Dalton, J.B., Grinspoon, D., Wattson, R.B., Freedman, D., Crisp, D., Allen, D.A., Bézard , B., de Bergh, C., Giver, L.P., Ma, Q., and Tipping, R., 1993. Near infrared light

from Venus' nightside: a spectroscopic analysis. Icarus **103,** 1-42.

Ragent, B. and Blamont,J., 1980. The structure of the clouds of Venus: Results of the Pioneer Venus nephelometer experiment. J.Geophys. Res., 85(A13):8089-8106.

Revercomb, H.E., Sromovsky,L.A., Suomi, V.E., and Boese, R, 1985. Net thermal radiation in the atmosphere of Venus. Icarus, 61:521-538.

Rossow, W.B., Del Genio,A.D., Limaye,S.S., and Travis, L.D., 1980. J. Geophys. Res. 85 8107-8128.

Seiff, A., et al., 1980. Measurements of thermal structure and thermal contrasts in the atmosphere of Venus: results from the four Pioneer Venus probes. J. Geophys. Res. 85 7903-7933.

Taylor, F.W., Beer, R., Chahine, M.T., Diner, D.J., Elson, L.S., Haskins, R. D. , McCleese, D.J.., Martonchik, J.V., Reichley, P.E., Bradley, S.P., Delderfield, J., Schofield, J.T., Farmer, C.B., Froidevaux, L., Leung, J., Coffey, M.T., and Gille, J.C., 1980. Structure and meteorology of the middle atmosphere of Venus : infrared remote sounding from the Pioneer Orbiter. *J. Geophys. Res,* **85,** 7963-8006.

Taylor, F.W. Carbon Monoxide In The Deep Atmosphere Of Venus. *Adv. Space Res.*, **16,** 6, 81-88, 1995.

Tomasko, M.G., Smith, P.H., Suomi, Venus.E., Stromovsky, L.A., Revercomb, H.E., Taylor, F.W., Seiff, A., Boese, R., Pollack, J.B., Ingersoll, A.P., Schubert, G., Covey, C.C., 1980. The thermal balance of Venus in the light of the Pioneer Venus mission. *J. Geophys. Res.*, **85,** 8187-8199.

Venus 1, eds Hunten, D.M., Colin, L., Donahue, T.M. and Moroz, V.I., 1983. U. Arizona Press.

von Zahn, U., Kumar, S., Niemann, H., and Prinn, R., 1983. Composition of the Venus atmosphere. In Venus (eds Hunten, D.M., Colin, L., Donahue, T.M. and Moroz, V.I.) 299-430.

Young, L.D.G., Young, A.T., and Zasova, L.V., 1984. A new interpretation of the Venera 11 spectra of Venus. Icarus, **60,** 138-151.

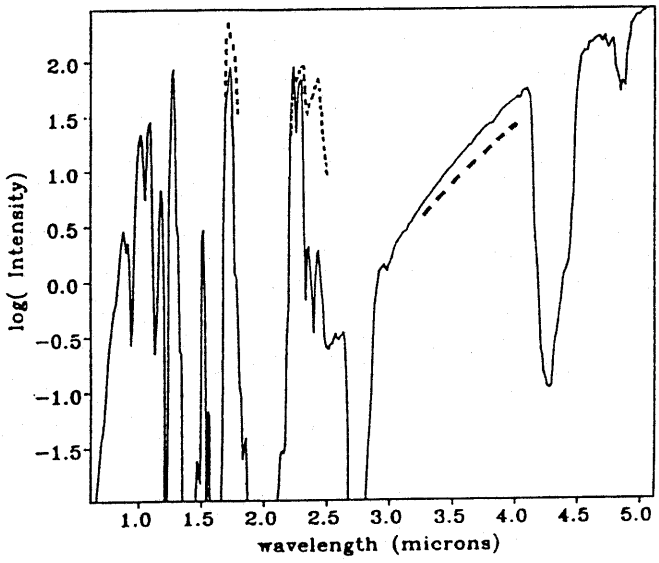

Fig.1 Early observed (dashed lines, Allen and Crawford, 1984) and modelled (solid line, Kamp et al., 1988) spectra for the night side of Venus.

Fig.2 The dark side of Venus, mapped at a wavelength of 2.3 μm in one of the most prominent of the near-IR 'windows'. It shows the highly variable nature of the opacity in the main cloud deck, illuminated from behind by thermal emision from the lower atmosphere. This view was obtained by the Near Infrared Mapping Spectrometer (NIMS) during the Galileo flyby of Venus on 10 February 1990 (Carlson et al., 1993).

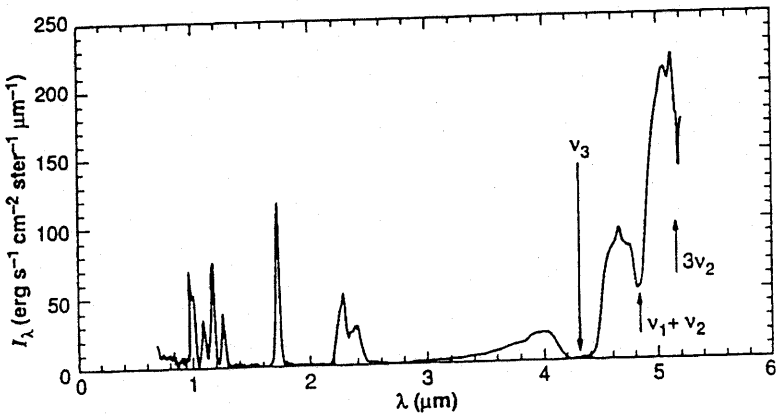

Fig.3 A representative spectrum of the dark side of Venus obtained by the NIMS instrument during the 1990 Galileo flyby (Carlson et al., 1991). The positions of some of the strongest CO_2 bands, which appear in absorption at the longer wavelengths, are indicated.

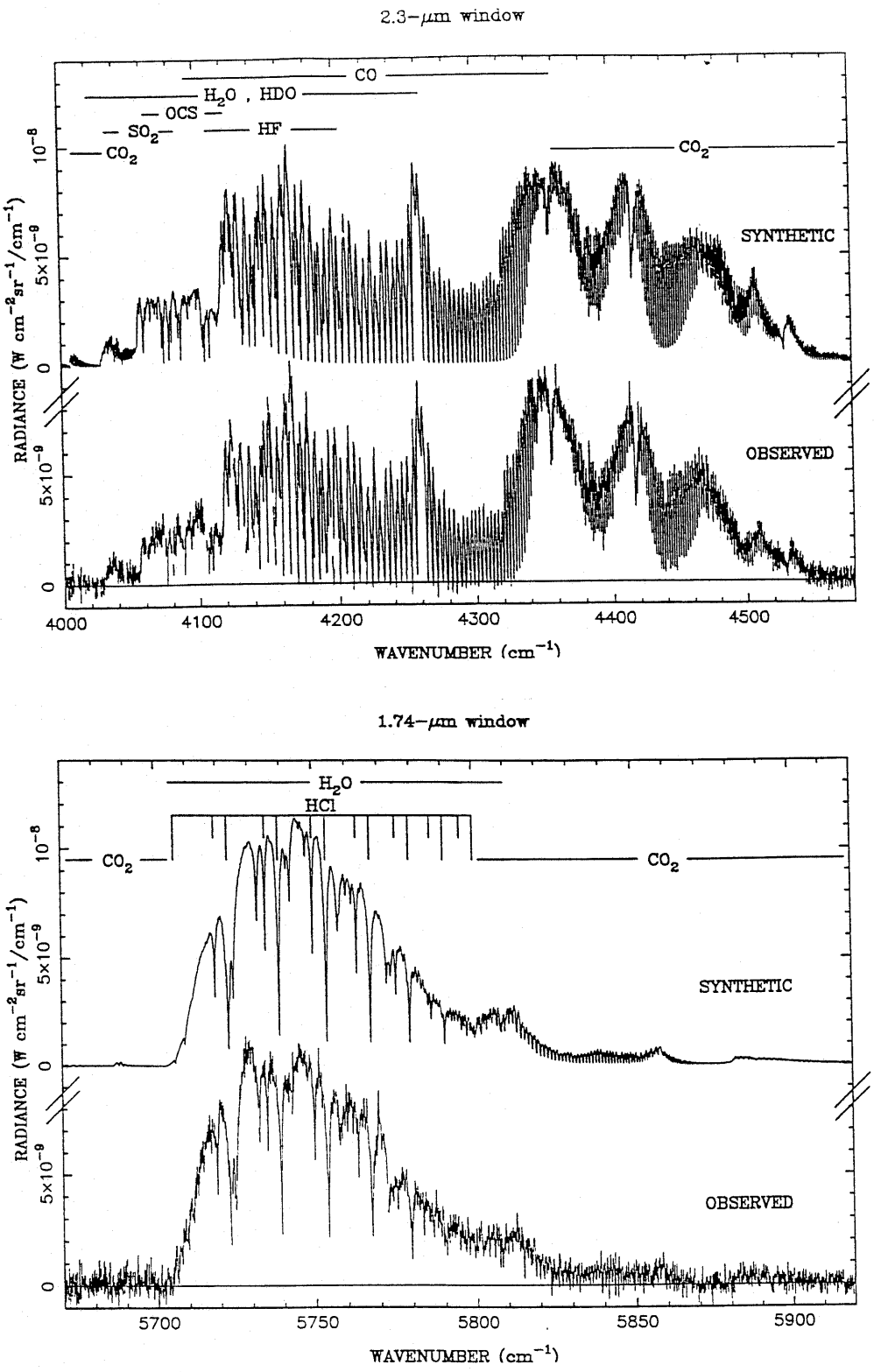

Fig. 4 High resolution ground-based spectra of the night side of Venus in (a) the 2.3 μm and (b) the 1.7 μm windows, with the main absorption features identified (Bézard, 1994).

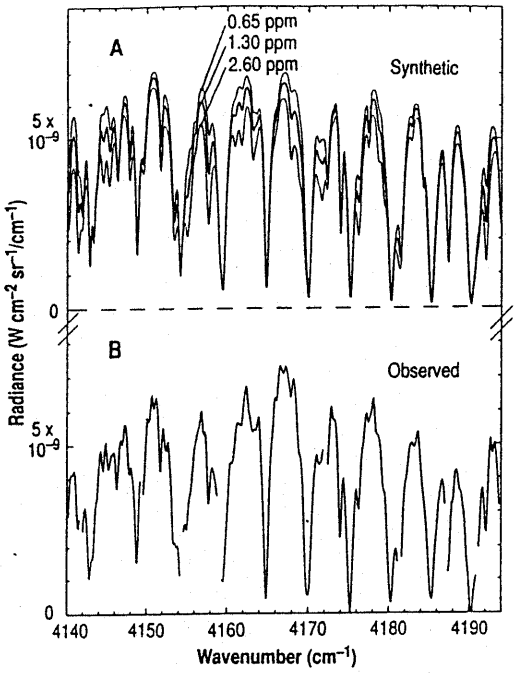

Fig. 5 Groundbased spectra of Venus showing the sensitivity to the mixing ratio of HDO. The best fit between computed and measured spectra is for 1.30 ppmv of HDO and 34 ppmv of H_2O. After de Berg et al. (1991).

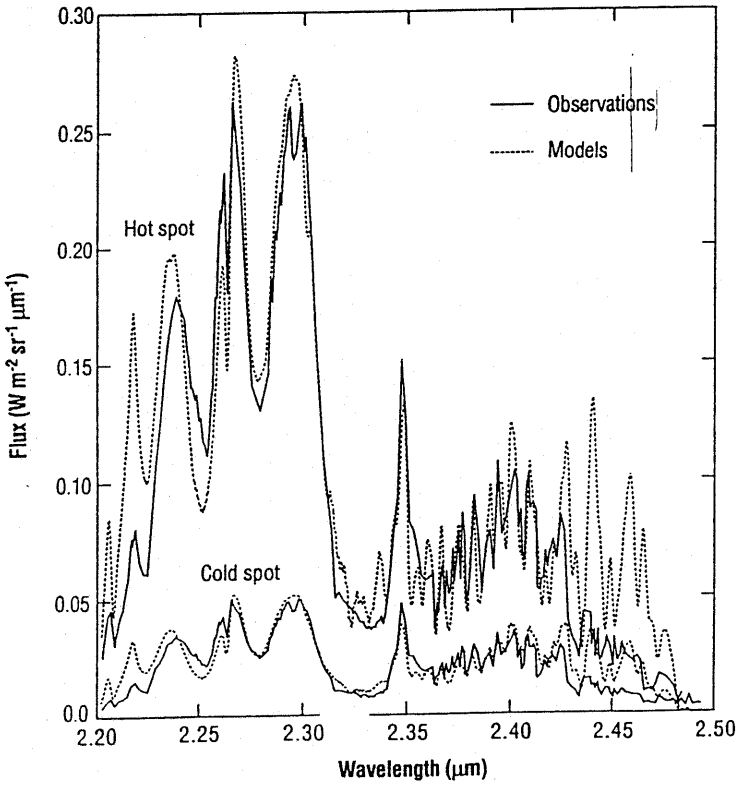

Fig.6 Spectra of hot and cold regions on Venus, with model fits (Bell et al. (1991). The amount of water vapour required to achieve a good fit was substantially different for the two regions.

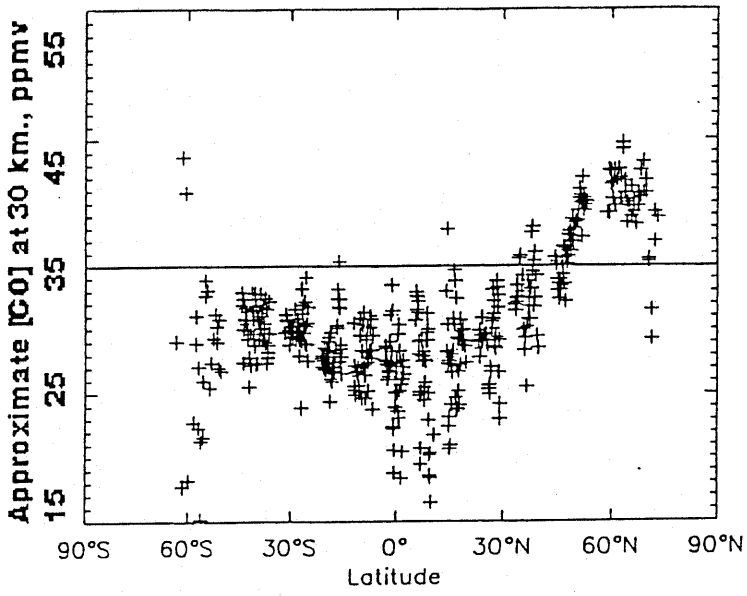

Fig.7 The distribution of carbon monoxide with latitude, inferred from the 0-2 band observed near 2.3 μm by Galileo-NIMS (after Collard et al., 1993 and Taylor, 1995). The abundance scale refers to the mean mixing ratio in a broad layer about 20 km thick centred on about 40 km altitude.

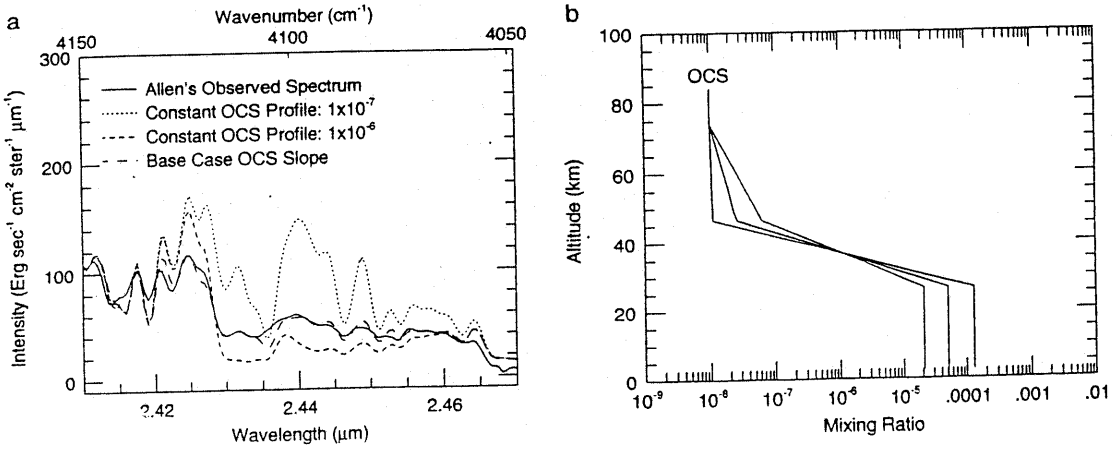

Fig.8 (Left) Observed and measured spectra in the 2.3 μm window showing features due to carbonyl sulfide (OCS). (Right) The range of OCS vertical profiles which provide a possible fit to the spectra. From Pollack et al., 1993.

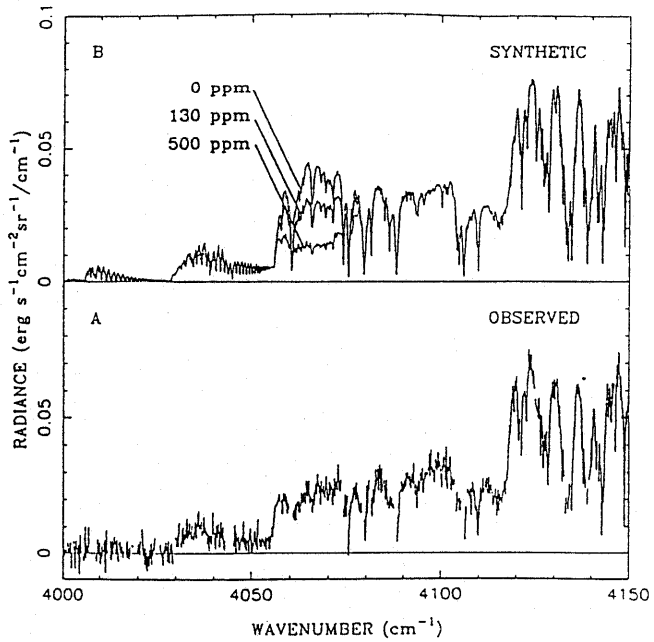

Fig.9 Observed and synthetic spectra for a region near 2.45 μm containing the $3\nu_3$ band of SO_2, showing the best fit value of 130 ppmv and the effect on the spectrum of varying this from 0 to 500 ppmv. From Bézard et al. (1993).